

Content-Based Search for Deep Generative Models

DAOHAN LU*, Carnegie Mellon University, USA
 SHENG-YU WANG*, Carnegie Mellon University, USA
 NUPUR KUMARI*, Carnegie Mellon University, USA
 ROHAN AGARWAL*, Carnegie Mellon University, USA
 MIA TANG, Carnegie Mellon University, USA
 DAVID BAU, Northeastern University, USA
 JUN-YAN ZHU, Carnegie Mellon University, USA

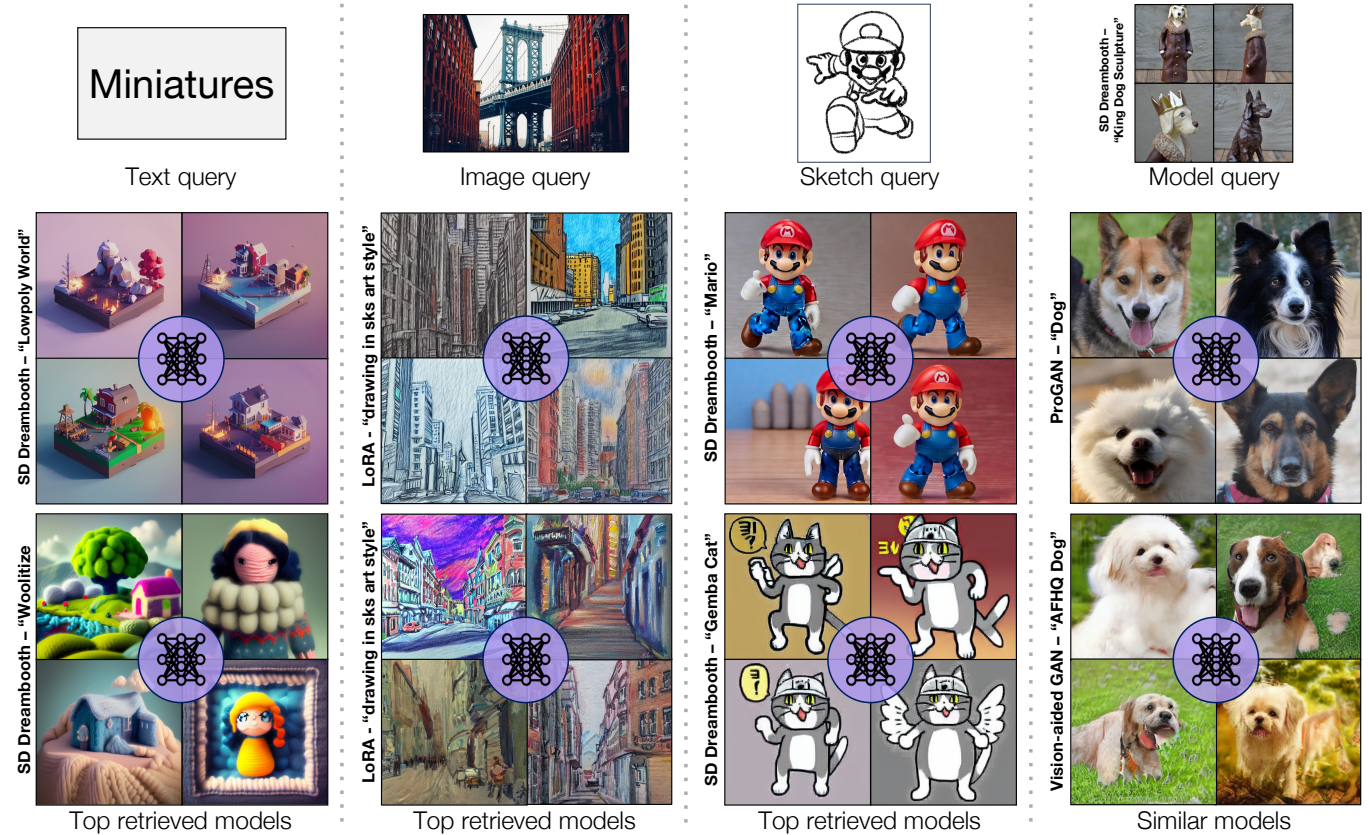


Fig. 1. We develop a search algorithm for customized and pre-trained deep generative models. We collect a diverse set of models, such as animals, landscapes, human faces, and art pieces. From left to right, our search algorithm enables queries in four modalities: text, images, sketches, and existing models. The 1st row consists of the queries, and the 2nd and 3rd rows show the first- and second-ranked models by our method, respectively. Our method succeeds in finding relevant models with similar semantic concepts across all four modalities. Different colors denote different model types. Photograph by @12019 on Pixabay.

The growing proliferation of customized and pretrained generative models has made it infeasible for a user to be fully cognizant of every model in existence. To address this need, we introduce the task of *content-based model search*: given a query and a large set of generative models, finding the models that best match the query. As each generative model produces a distribution of images, we formulate the search task as an optimization problem to select the model with the highest probability of generating similar content as the query. We introduce a formulation to approximate this probability given the query from different modalities, e.g., image, sketch, and text. Furthermore, we propose a contrastive learning framework for model retrieval, which learns to adapt features for various query modalities. We demonstrate that

our method outperforms several baselines on *Generative Model Zoo*, a new benchmark we create for the model retrieval task.

CCS Concepts: • **Computing methodologies** → **Artificial intelligence; Machine learning.**

Additional Key Words and Phrases: Imaging & Video, Machine Learning, Artificial Intelligence

* indicates equal contribution

1 INTRODUCTION

We introduce the task of content-based model search, which aims to find the most relevant deep image generative models that satisfy a user’s input query. For example, as shown in Figure 1, we enable a user to retrieve a model capable of synthesizing images that match a text query (e.g., Miniatures), an image query (e.g., a landscape photo), sketch query (e.g., Mario sketch), or models similar to a given model. Users can leverage retrieved models in various ways: they might further fine-tune it with a unique concept, use the model to generate an image with a more concrete prompt, or combine multiple retrieved models into one.

Content-based model search is becoming a vital task as the number and diversity of intriguing generative models continue to explode. These models have formed a new form of media content that requires efficient indexing and searching. While one might have expected large-scale text-to-image models [Ramesh et al. 2022; Rombach et al. 2022; Saharia et al. 2022] to have led to a shrinking universe of useful models, instead, this powerful class of content generators has touched off an accelerating proliferation of new and customized models. That is because powerful generative models are capable of being adapted to capture a wide range of personalized subjects [Gal et al. 2023; Kawar et al. 2023; Kumari et al. 2023; Ruiz et al. 2022]. Everyday users are routinely creating new generative models, and the community has collectively shared *tens of thousands* of custom models on community-driven platforms, such as Civitai [civ 2022] and HuggingFace [hug 2022] in the past year alone. Many popular models arise from the model creators’ unique creative processes, involving careful selections of subjects, algorithms, hyperparameters, and often proprietary artistic training data. Furthermore, some model creators receive compensation when other users download or use their models.

Aside from personalized models, a variety of deep generative models are being created as backbones for computer graphics applications [Bermano et al. 2022; Tewari et al. 2020], and as works of art that explore a wide range of themes [Elgammal 2019; Hertzmann 2020]. Each model captures a small universe of curated subjects, which can range from the realistic rendering of faces and landscapes [Karras et al. 2021] to photos of historic pottery [Au 2019] to cartoon caricatures [Jang et al. 2021] to single-artist stylistic elements [Schultz 2020]. Various methods also enable creative modifications of existing models via human-in-the-loop interfaces [Bau et al. 2020; Gal et al. 2022b; Wang et al. 2022].

Given the accelerating pace at which generative models are being created and uploaded to the internet, the ability to conduct content-based model search will be instrumental in supporting the effective use of large model collections. Existing model-sharing platforms [civ 2022; hug 2022] primarily rely on matching human-created model names for model search. However, it is difficult to choose sufficiently detailed names to describe the unique, complex, and highly specific images produced by a generative model. Our work aims to define a new approach, searching for models directly based on their content rather than based on manual definitions alone.

Content-based model search is a challenging task: even the simplified question of whether a specific image can be produced by a single model can be computationally difficult. Unfortunately, many

generative models do not offer an efficient or exact way to estimate density, nor do they natively support assessing cross-modal similarity (e.g., text and image).

To address the above challenges, we first curate a benchmark retrieval dataset, the Generative Model Zoo, consisting of (1) 259 publicly available generative models that vary in content as well as model architectures, including GANs (e.g., StyleGAN-family models [Karras et al. 2020b]), diffusion models (e.g., DreamBooth [Ruiz et al. 2022]), and auto-regressive models (e.g., VQGAN [Esser et al. 2021]) and (2) 1000 customized text-to-image diffusion models, each one fine-tuned on a single instantiation of an object class or a single artistic image. As part of our benchmark, we define ground truth image, text, and sketch queries for evaluating model retrieval.

We present a general probabilistic formulation of the model search problem and propose a learning-based method given this formulation. We summarize our contribution as follows:

- We introduce a new task of content-based search over deep generative models. Given a piece of text, an image, a sketch, a generative model, or a combination of them as a query, we aim to return the most relevant generative models that can synthesize similar content.
- We formulate the task of content-based model retrieval as estimating the probability of generating an image that matches the query content. We propose a new contrastive learning method to estimate the same given the model’s image distribution statistics and query. Our learning-based method outperforms several baseline algorithms.
- We curate a benchmark dataset, the Generative Model Zoo, which includes a diverse compilation of more than 250 community-created generative models, 1000 single-image fine-tuned models, and a set of ground truth (query, model) pairs for evaluating the retrieval algorithm on different query modalities.

2 RELATED WORKS

Deep generative models. Generative models are open-sourced at a rate of thousands per month. They use different learning objectives [Goodfellow et al. 2014; Ho et al. 2020; Kingma and Welling 2014; Oord et al. 2016; Song et al. 2021b], training techniques [Karras et al. 2020a; Mokady et al. 2022; Rombach et al. 2022; Sauer et al. 2021], and network architectures [Brock et al. 2019; Esser et al. 2021; Karras et al. 2019; Razavi et al. 2019]. They are also trained on different datasets [Choi et al. 2020; Mokady et al. 2022; Schultz 2020; Yu et al. 2015] for different applications [Albahar et al. 2021; Chen et al. 2020; Ha and Schmidhuber 2018; Lewis et al. 2021; Patashnik et al. 2021; Zhang et al. 2021; Zhu et al. 2021]. This diversity leads to the question, among all the models, which one shall we use? Our goal is *not* to introduce a new model. Instead, we want to help researchers, students, and artists find existing models more easily.

Model editing and fine-tuning. As methods for editing and fine-tuning generative models become more accessible and efficient, these have also contributed to a proliferation of models. Several works edit a pre-trained generative model with simple user interfaces like sketching [Wang et al. 2021], warping [Wang et al. 2022], blending [Bau et al. 2020], and text prompts [Gal et al. 2022b]. Besides editing a model, a line of works propose methods to fine-tune

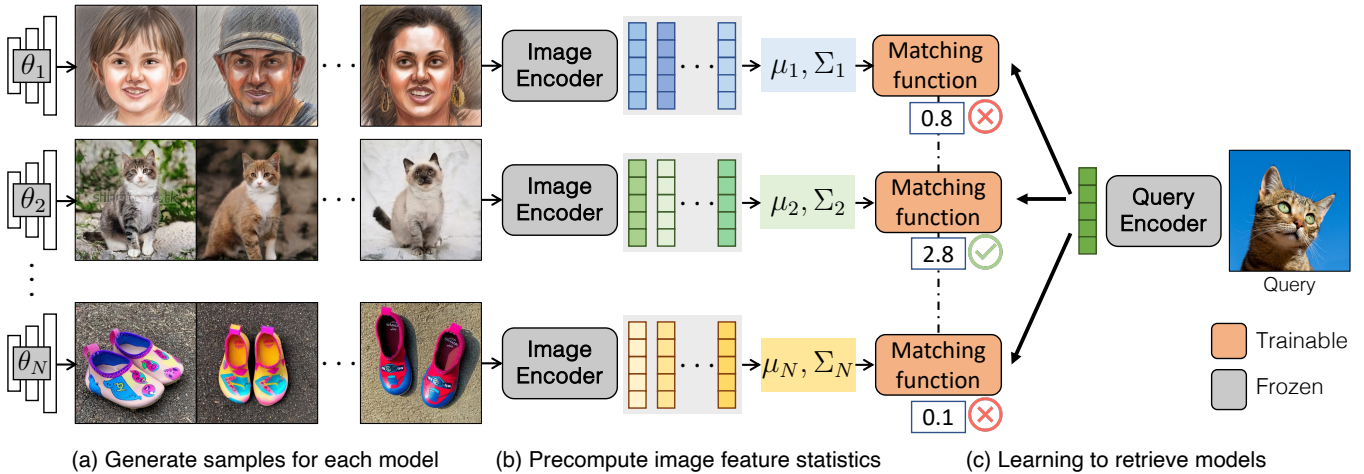


Fig. 2. **Overview.** Given a collection of models $\theta \sim \text{unif}\{\theta_1, \theta_2, \dots, \theta_N\}$, (a) we first generate samples for each model θ , and (b) encode the samples into features and compute the 1st and 2nd order feature statistics for each model. The statistics are cached for efficiency. (c) We then learn a matching function using contrastive loss that takes as input the query feature and model statistics and returns the similarity score between the model and query. The models with the best similarity scores are retrieved. We support queries of different modalities (text, image, or sketch). Photo by @cedric_photography (right).

models to match a small collection of images [Karras et al. 2020a; Li et al. 2020; Mo et al. 2020; Nitzan et al. 2022; Noguchi and Harada 2019; Ojha et al. 2021; Wang et al. 2020, 2018; Zhao et al. 2020a,b]. Various works further improve the fine-tuning speed [Grigoryev et al. 2022; Kumari et al. 2022; Liu et al. 2021; Sauer et al. 2021].

Customization of large-scale diffusion models. Recently, large-scale text-to-image models [Ramesh et al. 2022; Rombach et al. 2022; Saharia et al. 2022] have shown exemplary performance in generating diverse styles and compositions given the text prompt, with downstream versatile image editing capacity [Avrahami et al. 2022; Brooks et al. 2023; Hertz et al. 2022; Tumanyan et al. 2023; Zhang et al. 2023]. But these models cannot still synthesize personalized and artistic concepts that are hard to describe via text. To enable that, various works have proposed model customization techniques [Gal et al. 2022a; Han et al. 2023; Kawar et al. 2023; Kumari et al. 2023; Ruiz et al. 2022]. This has given rise to tens of thousands of fine-tuned models for different styles and concepts [civ 2022; hug 2022], thus making model search increasingly relevant. Recently, several works use retrieval-augmented generative models to improve the fidelity of rare entities [Blattmann et al. 2022; Casanova et al. 2021; Chen et al. 2023; Ma et al. 2023]. Different from these, our goal is to simply find a model relevant to user queries, rather than generating an exact image given the query.

Content-based retrieval. Building upon classical information retrieval [Baeza-Yates et al. 1999; Manning et al. 2010], content-based retrieval deals with queries over image, video, or other media [Datta et al. 2008; Gudivada and Raghavan 1995; Hu et al. 2011]. Content-based image retrieval methods use robust visual descriptors [Dalal and Triggs 2005; Lowe 2004; Oliva and Torralba 2001] to match objects within video or images [Arandjelović and Zisserman 2012; Sivic and Zisserman 2003]. Methods have been developed to compress visual features to scale retrieval [Gong et al. 2012; Jégou et al.

2010; Torralba et al. 2008; Weiss et al. 2008], and deep learning has enabled compact vector representations for retrieval [Babenko et al. 2014; Krizhevsky and Hinton 2011; Torralba et al. 2008; Zheng et al. 2017]. In addition to image queries, various works have proposed methods for sketch-based retrieval [Eitz et al. 2010; Lin et al. 2013; Liu et al. 2017; Radenovic et al. 2018; Ribeiro et al. 2020; Sangkloy et al. 2016; Yu et al. 2016]. There is a growing interest in joint visual-language embeddings [Faghri et al. 2017; Frome et al. 2013; Jia et al. 2021; Karpathy et al. 2014; Radford et al. 2021; Socher et al. 2014] that enable text queries for image content. We also adopt deep image representations for our setting, but unlike single-image retrieval, we index *distributions* of images that cannot be fully materialized. Concurrent to our work, HuggingGPT [Shen et al. 2023] also explores model retrieval but for user-defined tasks such as object detection.

3 METHODS

In this section, we develop a retrieval framework for deep generative models. When a user specifies an image, sketch, or text query, we would like to retrieve a model that best matches the query. We denote a collection of N models by $\{\theta_1, \theta_2, \dots, \theta_N\}$ and the user query by q , and we assume a uniform prior over models (i.e., $\theta \sim \text{unif}\{\theta_1, \theta_2, \dots, \theta_N\}$). Every model θ captures a distribution $p(x|\theta)$ over images x . While prior retrieval methods [Manning et al. 2010; Smeulders et al. 2000] search for single instances, we aim to construct a method for retrieving distributions.

To achieve this, we introduce a probabilistic formulation for generative model retrieval. Figure 2 shows an overview of our approach. Our formulation is general to different query modalities and various types of generative models, and can be extended to different algorithms. In Section 3.1, we derive our model retrieval formulation based on a Maximum Likelihood Estimation (MLE) objective based on pre-trained deep learning features. In Section 3.2, we further

propose a contrastive learning method to adapt features to different query modalities and model search task. We present our model retrieval algorithms for an image, a text, and a sketch query, respectively. In Sections 4 and 5, we discuss our new benchmark and user interface for model search.

3.1 Probabilistic Retrieval for Generative Models

Our goal is to quantify the posterior probability of each model θ given the user query q , and retrieve the model with the maximum $p(\theta|q)$. We define the probabilistic model retrieval objective as:

$$\max_{\theta \in \{\theta_1, \dots, \theta_N\}} p(\theta|q) = \frac{p(q|\theta)p(\theta)}{p(q)} \propto \max_{\theta \in \{\theta_1, \dots, \theta_N\}} p(q|\theta). \quad (1)$$

As we assume models are uniformly distributed, it is equivalent to finding the likelihood of the query under each model, $p(q|\theta)$.

There are two scenarios for inferring the query likelihood $p(q|\theta)$: (1) When the query q shares the same modality with the model θ (e.g., searching models with image queries), we directly reduce the problem to estimating the model's density. (2) When the query q has a different modality from the model θ (e.g., searching models with text queries), we use cross-modal similarity to estimate $p(q|\theta)$. We discuss both cases in the following.

Image-based model retrieval. Given an image query q , we directly estimate the likelihood of the query $p(q|\theta)$ from each model. In other words, we seek to find the model that is most likely to generate the query image. Since density estimation is intractable for many generative models (e.g., GANs [Goodfellow et al. 2014], VAEs [Kingma and Welling 2014]), we approximate each model as a Gaussian distribution over image features [Heusel et al. 2017]. After we sample an image from each model, denoted by x , we obtain its image feature $z := \phi_{im}(x)$, where ϕ_{im} is a frozen feature extractor. We now express $p(q|\theta)$ in terms of image features z , so Equation 1 becomes:

$$\max_{n \in \{1, \dots, N\}} (2\pi|\Sigma_n|)^{-\frac{1}{2}} \exp\left(-\frac{1}{2}(z_q - \mu_n)^T \Sigma_n^{-1} (z_q - \mu_n)\right), \quad (2)$$

where the query image feature is denoted by $z_q := \phi_{im}(q)$, and each model θ_n is approximated by $p(z|\theta_n) \sim \mathcal{N}(\mu_n, \Sigma_n)$. We refer to this method as Gaussian Density.

Text-based model retrieval. Given a text query q and a generative model $p(x|\theta)$ capturing a distribution of images x , we want to estimate the conditional probability $p(q|\theta)$.

$$p(q|\theta) = \int p(q|x)p(x|\theta)dx \propto \int \frac{p(x|q)}{p(x)} p(x|\theta)dx. \quad (3)$$

Here we assume conditional independence between query q and model θ given image x , so $p(q|x, \theta) = p(q|x)$, and we apply Bayes' rule to get the final expression. In Equation 3, a text query q may correspond to multiple possible image matches $p(x|q)$, so the expression cannot be simplified the same way as image-based model retrieval. Instead, we can view Equation 3 as an integral of the mutual information between q and x , which can be estimated with a contrastive representation [Oord et al. 2018]. Thus, we use CLIP similarity [Radford et al. 2021] to approximate $\frac{p(x|q)}{p(x)} \propto \exp(\frac{1}{\tau} \tilde{h}_x^T \tilde{h}_q)$, where $\tilde{h}_x := \phi_{im}(x)$ and $\tilde{h}_q := \phi_{txt}(q)$ are the normalized CLIP image and text features; τ is a temperature term.

To approximate the integration, one can sample images x from $p(x|\theta)$ and then take the average of the CLIP similarities between images and query. We refer to this method as Monte-Carlo. To further speed up computation, we can pre-compute the mean of CLIP image embeddings for each model, and at inference time, we directly evaluate similarities between the query embedding and the mean embedding, as follows:

$$\int \frac{p(x|q)}{p(x)} p(x|\theta) dx \approx \exp\left(\frac{\tilde{\mu}_n^T \tilde{h}_q}{\tau}\right), \quad (4)$$

$$\text{where } \mu_n = \mathbb{E}_{\tilde{h}_x \sim p(\tilde{h}_x|\theta_n)} [\tilde{h}_x]; \tilde{\mu}_n = \frac{\mu_n}{\|\mu_n\|}.$$

We find that this approximation works well in practice, and we refer to this method as 1st Moment. Derivation details for Monte-Carlo and 1st Moment can be found in Appendix C.

1st Moment method for image queries. Likewise, we find that applying 1st Moment for image-based model retrieval yields a performance close to Gaussian Density. Interestingly, for sketch queries, 1st Moment method outperforms Gaussian Density. While CLIP shows strong cross-modal matching performance between sketch queries and image models, the domain gap makes density estimation a less favorable option for sketch queries compared to the 1st Moment method. We provide more discussions in Section 6.

3.2 Learning to Retrieve Models

We have outlined several ways to approximate $p(\theta|q)$ in Section 3.1 to perform content-based model retrieval. However, these approximations involve only pre-trained feature extractors and may not be optimal for model retrieval with certain query modalities. For example, the frozen features that work well for images may struggle with sketches. To address this issue, we introduce a set of learnable parameters to fine-tune the approximations of $p(\theta|q)$ on our Generative Model Zoo dataset (Section 4).

Under the contrastive learning framework, we maximize $\mathbb{E}\left[\log \frac{p(\theta|q)}{p(\theta)}\right]$, the mutual information between the query q and the model θ . Since we assume a uniform prior over the models, the mutual information is effectively our retrieval objective $\mathbb{E}[\log p(\theta|q)]$. The training dataset \mathcal{D} consists of sample statistics for M models and a number of ground-truth query-model pairs. We optimize a matching function s_ψ that yields a query-to-model similarity score, by minimizing the InfoNCE loss [Oord et al. 2018]:

$$\min_{\psi} \mathbb{E}_{(q, \theta_i) \sim \mathcal{D}} \left[-\log \frac{\exp(s_\psi(q, \theta_i)/\tau)}{\sum_{j=1}^M \exp(s_\psi(q, \theta_j)/\tau)} \right], \quad (5)$$

$$s_\psi(q, \theta_i) = \begin{cases} \frac{(A_\psi \tilde{\mu}_i)^T (A_\psi \tilde{h}_q)}{\|A_\psi \tilde{\mu}_i\| \|A_\psi \tilde{h}_q\|} & \text{if 1st Moment} \\ \log \mathcal{N}(\tilde{h}_q | \mu_i, A_\psi \Sigma_i A_\psi^T) & \text{if Gaussian Density} \end{cases} \quad (6)$$

where A_ψ is a matrix parameterized by ψ , (μ_i, Σ_i) are the feature-space sample mean and covariance of model θ_i , and \tilde{h}_q is as calculated in the previous section using a pre-trained feature extractor. The contrastive learning objective maximizes the similarity score between query q and the ground truth model and minimizes the similarity between the query and other models.

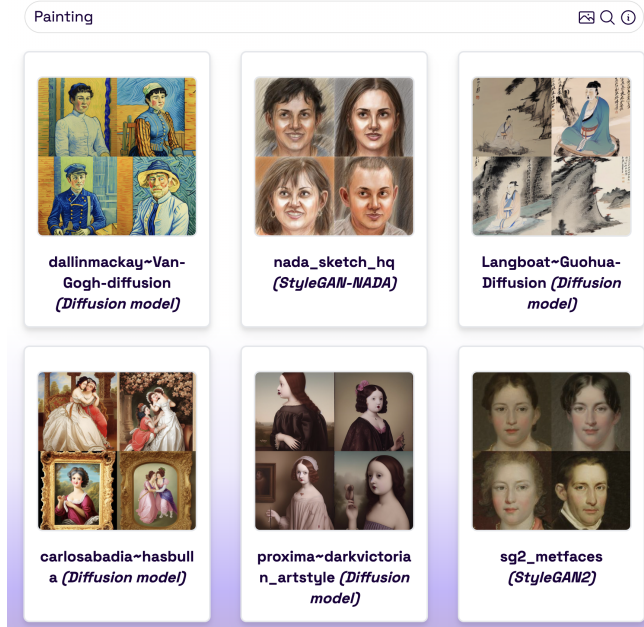


Fig. 3. **User interface.** In our model search platform, a user can submit a text query, an image query, or a combination of both to retrieve generative models that best match the query. Here we show the top 6 retrievals for the text query “painting”. The user can further explore additional samples from the models or search for models similar to a particular model.

We define the matching function based on two formulations described in Section 3.1: 1st Moment and Gaussian Density. For 1st Moment, we project the original feature using the matrix A_ψ . For Gaussian Density, $\mathcal{N}(\tilde{h}_q|\mu_i, A_\psi\Sigma_iA_\psi^T)$ denotes the gaussian PDF with parameters $\{\mu_i, A_\psi\Sigma_iA_\psi^T\}$, evaluated at the query feature \tilde{h}_q . We experiment with different A_ψ parameterizations, including full, triangular, and diagonal matrices. For the diagonal case, we limit the range of A_ψ such that $A_\psi = \text{diag}(\text{sigmoid}(\psi))$

In Section 6, we show that our method can retrieve models that share similar visual concepts with the query.

4 THE GENERATIVE MODEL ZOO

We introduce a new benchmark, the Generative Model Zoo, consisting of a set of generative models capturing a variety of architectures and subject areas for evaluating retrieval performance.

Internet model zoo. It consists of a total of 259 publicly available generative models trained using different techniques, including GANs [Gal et al. 2022b; Karras et al. 2018, 2021, 2020b; Kumari et al. 2022; lucid layers 2022; Mokady et al. 2022; Pinkney 2020; Sauer et al. 2022; Wang et al. 2021, 2022], diffusion models [Dhariwal and Nichol 2021; Ho et al. 2020; Ruiz et al. 2022; Song et al. 2021a], MLP-based generative model CIPS [Anokhin et al. 2021], and the autoregressive model VQGAN [Esser et al. 2021]. Out of the 259 models, 23 were created via fine-tuning by individual users, 133 were obtained from the GitHub repositories of academic papers, and the remaining models were collected from public model sharing

website [hug 2022]. This includes models like DreamBooth [Ruiz et al. 2022] that are finetuned to generate a specific concept (e.g., a unique toy) with a fixed text prompt as input. Hence, to index these models, we generate samples conditioned on the unique text prompt used to fine-tune the model. A comprehensive list of the models and their respective sources is included in Appendix B.

We create a set of benchmark queries for each model in multiple modalities, i.e., text, image, and sketch. The text queries include human-written textual queries that describe the images in a model. Image queries are created by sampling images from models, and sketch queries are created by using the method of Chan *et al.* [2022].

Synthetic model zoo. To further test our method at scale, we create a synthetic model zoo of 1,000 models. Each model is finetuned from the pretrained Stable Diffusion v1.4 checkpoint [Rombach et al. 2022] on a single image. The models are fine-tuned on instances from animal classes in ImageNet [Deng et al. 2009] or artistic images downloaded from Unsplash [Unsplash 2022]. We manually pick 50 ImageNet classes and 10 instance images from each class, thus training 500 models with instance images from the ImageNet Dataset. For the artistic models, we select 500 images from Unsplash that match the keyword “art”. To fine-tune the model, we randomly select between Dreambooth [Ruiz et al. 2022] with LoRA [Hu et al. 2021] and Custom Diffusion [Kumari et al. 2023]. In this case, we only create image and sketch queries, as describing specific instantiation of a general category from ImageNet classes is difficult via only text. Similarly, describing an art work using text is also non-trivial.

5 USER INTERFACE

Our baseline method is fast enough for interactive use, and we create a web-based UI for the search algorithm. The user can search for models by entering text or uploading an image/sketch. The interface displays models that best match the query, where clicking on a model’s thumbnail shows more image samples. The website utilizes a backend GPU server to enable real-time model search on any client device. Figure 3 shows a screenshot of our UI.

6 EXPERIMENTS

For our baseline retrieval methods, we benchmark their performance over text, image, and sketch modalities and discuss several algorithmic design choices.

Implementation details. We test our method with the commonly used pretrained feature extractor – CLIP [Radford et al. 2021]. We use the ℓ_2 -normalized CLIP features, as discussed in Section 3.1.

We pre-calculate each model’s generated distribution mean and covariance in the CLIP feature space, following the pre-processing steps described in clean-fid [Parmar et al. 2022]. For ImageNet fine-tuned models, we generate class-specific prompts used to sample images using ChatGPT. For artistic fine-tuned models, we use general prompts, e.g., “a painting in the style of <specific art style>”. More implementation details are in Appendix B.

To evaluate model search, we use the top-k accuracy metric, i.e., frequency of finding the *unique* ground truth model within the top-k retrieved models using the query corresponding to that model.

Table 1. **Image- and sketch-based model retrieval.** We compare retrieval performance with pre-trained and fine-tuned scoring functions utilizing CLIP network backbone. We observe the best performance with CLIP and fine-tuning. The (FT) suffix denotes the learning-based method (Equation 6) using the optimal parameterization selected via first doing cross-validation on the *Synthetic Model Zoo* as shown in Table 2.

		Top-k Accuracy		
		Top-1	Top-5	Top-10
Image (Gen.)	CLIP+Monte-Carlo (2.4K)	0.82	0.96	0.99
	CLIP+best-k (2.4K, k=1)	0.80	0.95	0.99
	CLIP+best-k (2.4K, k=10)	0.82	0.96	0.99
	CLIP+1 st Moment	0.78	0.94	0.98
	CLIP+1 st Moment (FT)	0.81	0.95	0.98
	CLIP+Gaussian Density	0.84	0.96	0.98
	CLIP+Gaussian Density (FT)	0.85	0.96	0.99
	CLIP+Monte-Carlo (2.4K)	0.32	0.59	0.72
Sketch	CLIP+best-k (2.4K, k=1)	0.28	0.55	0.68
	CLIP+best-k (2.4K, k=10)	0.32	0.59	0.72
	CLIP+1 st Moment	0.32	0.61	0.73
	CLIP+1 st Moment (FT)	0.49	0.75	0.84
	CLIP+Gaussian Density	0.18	0.39	0.53
	CLIP+Gaussian Density (FT)	0.30	0.56	0.69

6.1 Model Retrieval

Model retrieval via image and sketch queries. We report top-k accuracy of model retrieval on the *Internet model zoo* dataset in Table 1. We show the performance of different formulations with CLIP features. We train the transformation matrix A_ψ in the learning to retrieve method using the *Synthetic model zoo*. The retrieval performance is best with CLIP features combined with our learning method, especially for sketch-based retrieval. The learning method is denoted with the suffix (FT) in Table 1. For comparison, we also include a modified k-NN algorithm in which we find the query’s feature-space k-nearest neighbors among each model’s image samples and sort the models by the mean distance to those k samples. We refer to this baseline as “best-k neighbors” or simply “best-k”. Figure 7 shows qualitative examples of model retrieval for different image and sketch queries.

Learning to retrieve models. We conduct 5-fold cross-validation on *Synthetic Model Zoo* to determine the best parameterization of the transformation matrix A_ψ for the learnable matching function (Equation 6). Table 2 shows the test-set top-1 accuracy of each method compared to the baseline, which uses the pre-trained feature extractor. We find that our contrastive learning method consistently improves the pretrained features for various query modalities and formulations. We select the best parameterization via cross-validation for training the matching function from scratch on the full *Synthetic Model Zoo* and then test on the *Internet Model Zoo*. The learned matching function generalizes to the *Internet Model Zoo* as shown in Table 1. We also train our method on *Internet Model Zoo*

Table 2. **Selecting best parameterization for A_ψ with cross-validation.** We fine-tune different versions of similarity function and transformation matrix parameterization with 5-fold cross-validation on the *Synthetic Model Zoo*. We use it to determine the optimal parameterization of A_ψ (marked with a “★”) for each method and modality.

			Mean Testing Accuracy		
			Top-1 (FT)	Top-1 (Pre-trained)	
	Modality	A_ψ			
Synthetic Zoo	CLIP+1 st Moment	Image	Diagonal	0.84	0.81
	CLIP+1 st Moment	Image	★Triangular	0.90	0.81
	CLIP+1 st Moment	Image	Full	0.89	0.81
	CLIP+Gaussian Density	Image	Diagonal	0.91	0.88
	CLIP+Gaussian Density	Image	★Triangular	0.91	0.88
	CLIP+Gaussian Density	Image	Full	0.91	0.88
	CLIP+1 st Moment	Sketch	Diagonal	0.30	0.15
	CLIP+1 st Moment	Sketch	★Triangular	0.61	0.15
	CLIP+1 st Moment	Sketch	Full	0.61	0.15
	CLIP+Gaussian Density	Sketch	Diagonal	0.29	0.09
	CLIP+Gaussian Density	Sketch	★Triangular	0.51	0.09
	CLIP+Gaussian Density	Sketch	Full	0.38	0.09

Table 3. **Learning to retrieve with text queries.** We show the result of the learning-based method with text queries using a 5-fold cross-validation on the *Internet Model Zoo* itself. This is because we have ground truth text queries only for that, as discussed in Section 4. We optimize different parameterizations of the transformation matrix on the training split and show retrieval performance on the testing split of 51 models.

			Mean Testing Accuracy		
			Top-1 (FT)	Top-1 (Pre-trained)	
	Modality	A_ψ			
Internet Zoo	CLIP+Monte-Carlo (2.4K)	Text	-	0.75	
	CLIP+best-k (2.4K, k=1)	Text	-	0.67	
	CLIP+best-k (2.4K, k=10)	Text	-	0.74	
	CLIP+1 st Moment	Text	Diagonal	0.78	0.77
	CLIP+1 st Moment	Text	Triangular	0.80	0.77
	CLIP+1 st Moment	Text	Full	0.81	0.77

and qualitatively test its generalization on *Synthetic Model Zoo* in Figure 8. Please refer to Appendix A for a quantitative analysis.

Text-based model retrieval. We show the results of text-based retrieval on *Internet Model Zoo*, i.e., collected publicly available generative models, which we manually labeled with corresponding text descriptions. We use the CLIP [Radford et al. 2021] as the pretrained feature extractor since CLIP has both text and image encoders. Since our learning-based method requires a training and test split, we perform 5-fold cross-validation and show the mean Top-1 accuracy for all methods, including baselines, to be consistent. Table 3 shows the retrieval performance of both methods. Similar to image and sketch-based retrieval, we also include results for the best-k neighbors baseline. The proposed baseline method achieves an accuracy of 77%, while the best learning-based method outperforms it with 81% accuracy.

Figure 7 shows qualitative examples of the top three and lowest-ranked retrieval given a text query with the 1st Moment method. Both quantitative numbers and visual inspection of results show that our method retrieves relevant generative models. We also analyze

the retrieval score of all models corresponding to a given query. For object categories, such as “dogs” or “buses”, we observe a clear drop in retrieval score for irrelevant models. For broader queries, such as “indoors”, “modern art” and “painting”, the drop-off is gradual. We show detailed analysis in Appendix A.

Comparison with metadata-based search. We compare against an alternative where we index models using user-defined descriptions and search for models by text-matching the query and the model descriptions. To test this, we use the text query associated with each model as its description (e.g., “portraits with Botero’s style” for one of the StyleGAN-NADA models).

We test metadata-based search on image- and sketch-based retrieval, with two ways of description-matching. (1) *Description (text)*: we caption image/sketch queries using BLIP [Li et al. 2022] and retrieve models whose descriptions contain any nouns, verbs, or adjectives (i.e., any non-filler words) that appear in the caption. (2) *Description (CLIP)*: we embed model descriptions into CLIP features and compare the similarity between the image/sketch query feature and the description feature.

As shown in Table 4, the content-based search methods outperform the baselines while they also obviate the need for model descriptions. Metadata-based search typically fails when captions are incorrect or when the object-centric tags cannot describe the model fully. Creating comprehensive descriptions might reduce the gap, but it is time-consuming to describe every visual aspect and anticipate users’ queries in advance. Our evaluation does not include text-based queries, as we use the model descriptions as the ground truth. However, we expect the baselines to have the same limitation for text queries in the case where a text query requests a visual concept that the tags fail to enumerate.

Running time and memory. Time and memory efficiency are crucial for supporting many concurrent user searches over a large-scale model collection. While 1st Moment obtains competitive top-k accuracies, it runs $3.2\text{-}7.5\times$ faster than Monte-Carlo or Gaussian Density. The fine-tuned 1st Moment method further improves accuracy, but runs at speeds more on par with Monte-Carlo or Gaussian Density. 1st Moment is extremely memory-efficient. Further analysis is in Appendix A.

7 EXTENSIONS

We describe two extensions: searching with multimodal queries and searching with a given model.

Multimodal user query. We show qualitatively that our search method can be extended to multimodal queries based on the Product-of-Experts formulation [Hinton 2002; Huang et al. 2022]. Given a multimodal query (e.g., text-image pair), the retrieval score is the product of individual query likelihoods. We demonstrate how one can leverage multiple input modalities to perform nuanced searches in Figure 4 using the 1st Moment method with pre-trained features. We show additional multimodal retrieval results in Appendix A.

Generative model query. Given the generative model collection, we can also retrieve similar models based on the cosine similarity between the feature-space means of query models and other generative models. Figure 5 shows qualitative examples of similar-model retrieval using CLIP feature space.

Table 4. **Comparison with metadata-based search.** We compare our Gaussian Density content-based search method with two metadata-based search methods: (1) *Description (text)*: we caption image/sketch queries using BLIP [Li et al. 2022] and select models whose descriptions contains any non-filler words from the caption, (2) *Description (CLIP)*, we embed model descriptions into the CLIP feature space and compare the similarity between the CLIP query features and the CLIP description features.

		Top-k Accuracy		
		Top-1	Top-5	Top-10
Image (Gen.)	Description (text)	0.07	0.20	0.29
	Description (CLIP)	0.45	0.72	0.85
	CLIP+Gaussian Density (ours)	0.89	0.98	0.99
Sketch	Description (text)	0.07	0.20	0.28
	Description (CLIP)	0.22	0.46	0.60
	CLIP+1 st Moment (ours)	0.49	0.75	0.84

8 DISCUSSION AND LIMITATIONS

We have introduced the new task of content-based generative model search. We have developed a data set for benchmarking model retrieval algorithms, and we have described several baselines and a contrastive learning method for further improving features.



Fig. 4. **Multi-modal user query.** Image and text queries combined can define nuanced concepts. When querying with the phrase “pointy eyes” plus a cat photo, we can retrieve “Triangle Eyes Cat” and “Alien Eyes Cat”. Photo by cocoparisienne on Pixabay.

Limitations. While we can retrieve models in real-time based on text, image, or sketch queries, our method has several limitations. First, while our method is able to successfully retrieve models that capture a single concept (e.g., StyleGAN3 [Karras et al. 2021] and DreamBooth [Ruiz et al. 2022]). There remain many future directions, including searching for personalized models that contain multiple subjects [Kumari et al. 2023], 3D neural objects [Mildenhall et al. 2021; Poole et al. 2022], and other media such as text, audio, and videos.

Second, our method can sometimes fail to match the user intent. A typical failure case is illustrated in Figure 6, where a query for a sketch of left facing horse retrieves general horse models instead of the most similar GANSketch “Left-facing Horse” model. It fails to respect the spatial orientation of the object in the query image. We show further analysis on this in Appendix A.

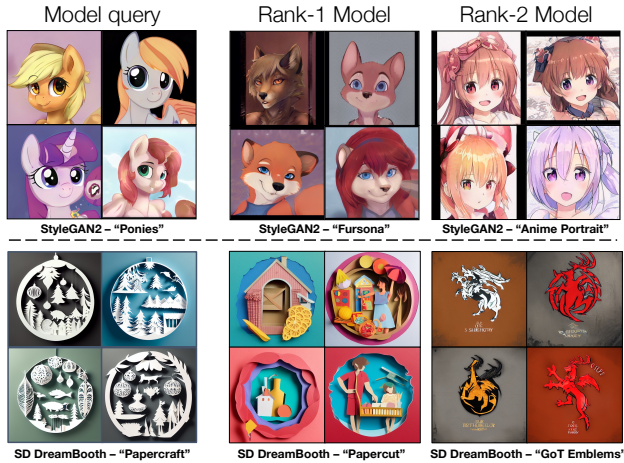


Fig. 5. **Finding similar models.** Our method can find models that share similar characteristics with the query model.



Fig. 6. **Limitation.** Sometimes, a sketch query (e.g., the left-facing horse sketch) does not retrieve the most similar model at the top, which should be the GANSketch "Left-facing Horse" model. Sketch by Damaris Dharmah on Pixabay.

Nevertheless, our experiments have shown that it is realistic, possible, and useful to search an indexed collection of models by matching them against the output behavior of the models. As the number of customized and pre-trained models continues to balloon, we anticipate that search algorithms that can effectively locate relevant customized models will be an increasingly valuable resource for researchers and content creators.

ACKNOWLEDGMENTS

We thank George Cazenavette, Gaurav Parmar, Chonghyuk (Andrew) Song, and Or Patashnik for proofreading the draft. We are also grateful to Aaron Hertzmann, Maneesh Agrawala, Stefano Ermon, Chenlin Meng, William Peebles, Richard Zhang, Phillip Isola, Taesung Park, Muyang Li, Kangle Deng, and Ji Lin for helpful comments and discussion. The work is partly supported by NSF IIS-2239076, Adobe Inc., Sony Corporation, and Naver Corporation.

REFERENCES

2022. Civit AI. <https://civitai.com>.
 2022. Stable Diffusion Dreambooth Concepts Library. <https://huggingface.co/sd-dreambooth-library>.

Badour Albahar, Jingwan Lu, Jimei Yang, Zhixin Shu, Eli Shechtman, and Jia-Bin Huang. 2021. Pose with Style: Detail-Preserving Pose-Guided Image Synthesis with Conditional StyleGAN. *ACM TOG* (2021).

Ivan Anokhin, Kirill Demochkin, Taras Khakhulin, Gleb Sterkin, Victor Lempitsky, and Denis Korzhenkov. 2021. Image Generators with Conditionally-Independent Pixel Synthesis. In *CVPR*.

Relja Arandjelović and Andrew Zisserman. 2012. Three things everyone should know to improve object retrieval. In *CVPR*.

Derek Philip Au. 2019. This vessel does not exist. <https://thisvesseldoesnotexist.com/>.

Omri Avrahami, Dani Lischinski, and Ohad Fried. 2022. Blended diffusion for text-driven editing of natural images. In *CVPR*.

Artem Babenko, Anton Slesarev, Alexandr Chigorin, and Victor Lempitsky. 2014. Neural codes for image retrieval. In *ECCV*.

Ricardo Baeza-Yates, Berthier Ribeiro-Neto, et al. 1999. *Modern information retrieval*. Vol. 463. ACM press New York.

David Bau, Steven Liu, Tongzhou Wang, Jun-Yan Zhu, and Antonio Torralba. 2020. Rewriting a deep generative model. In *ECCV*.

Amit H Bermano, Rinon Gal, Yuval Alaluf, Ron Mokady, Yotam Nitzan, Omer Tov, Or Patashnik, and Daniel Cohen-Or. 2022. State-of-the-Art in the Architecture, Methods and Applications of StyleGAN. *arXiv preprint arXiv:2202.14020* (2022).

Andreas Blattmann, Robin Rombach, Kaan Oktay, Jonas Müller, and Björn Ommer. 2022. Retrieval-augmented diffusion models. *Advances in Neural Information Processing Systems* 35 (2022), 15309–15324.

Andrew Brock, Jeff Donahue, and Karen Simonyan. 2019. Large scale gan training for high fidelity natural image synthesis. In *ICLR*.

Tim Brooks, Aleksander Holynski, and Alexei A Efros. 2023. Instructpix2pix: Learning to follow image editing instructions. In *Proceedings of the IEEE/CVF Conference on Computer Vision and Pattern Recognition*. 18392–18402.

Arantxa Casanova, Marlene Careil, Jakob Verbeek, Michal Drozdal, and Adriana Romero Soriano. 2021. Instance-conditioned gan. *Advances in Neural Information Processing Systems* 34 (2021), 27517–27529.

Caroline Chan, Fredo Durand, and Phillip Isola. 2022. Learning to generate line drawings that convey geometry and semantics. In *CVPR*.

Shu-Yu Chen, Wanchao Su, Lin Gao, Shihong Xia, and Hongbo Fu. 2020. DeepFace-Drawing: Deep generation of face images from sketches. *ACM Transactions on Graphics (TOG)* 39, 4 (2020), 72–1.

Wenhu Chen, Hexiang Hu, Chitwan Saharia, and William W Cohen. 2023. Re-imagen: Retrieval-augmented text-to-image generator. In *ICLR*.

Yunje Choi, Youngjung Uh, Jaemin Yoo, and Jung-Woo Ha. 2020. StarGAN v2: Diverse Image Synthesis for Multiple Domains. In *CVPR*.

Navneet Dalal and Bill Triggs. 2005. Histograms of oriented gradients for human detection. In *CVPR*.

Ritendra Datta, Dhiraj Joshi, Jia Li, and James Z Wang. 2008. Image retrieval: Ideas, influences, and trends of the new age. *ACM Computing Surveys (Csur)* (2008).

J. Deng, W. Dong, R. Socher, L.-J. Li, K. Li, and L. Fei-Fei. 2009. ImageNet: A Large-Scale Hierarchical Image Database. In *CVPR*.

Prafulla Dhariwal and Alexander Nichol. 2021. Diffusion models beat gans on image synthesis. In *NeurIPS*.

Mathias Eitz, Kristian Hildebrand, Tamy Boubekeur, and Marc Alexa. 2010. Sketch-based image retrieval: Benchmark and bag-of-features descriptors. *IEEE transactions on visualization and computer graphics* 17, 11 (2010), 1624–1636.

Ahmed Elgammal. 2019. AI is blurring the definition of artist: Advanced algorithms are using machine learning to create art autonomously. *American Scientist* 107, 1 (2019), 18–22.

Patrick Esser, Robin Rombach, and Björn Ommer. 2021. Taming transformers for high-resolution image synthesis. In *CVPR*.

Fartash Faghri, David J Fleet, Jamie Ryan Kiros, and Sanja Fidler. 2017. Vse++: Improving visual-semantic embeddings with hard negatives. In *BMVC*.

Andrea Frome, Greg S Corrado, Jon Shlens, Samy Bengio, Jeff Dean, Marc'Aurelio Ranzato, and Tomas Mikolov. 2013. Devise: A deep visual-semantic embedding model. In *NeurIPS*.

Rinon Gal, Yuval Alaluf, Yuval Atzmon, Or Patashnik, Amit H Bermano, Gal Chechik, and Daniel Cohen-Or. 2022a. An image is worth one word: Personalizing text-to-image generation using textual inversion. *arXiv preprint arXiv:2208.01618* (2022).

Rinon Gal, Moab Arar, Yuval Atzmon, Amit H Bermano, Gal Chechik, and Daniel Cohen-Or. 2023. Encoder-based domain tuning for fast personalization of text-to-image models. *ACM Transactions on Graphics (TOG)* 42, 4 (2023), 1–13.

Rinon Gal, Or Patashnik, Haggai Maron, Gal Chechik, and Daniel Cohen-Or. 2022b. StyleGAN-NADA: CLIP-Guided Domain Adaptation of Image Generators. *ACM TOG* (2022).

Yunchao Gong, Svetlana Lazebnik, Albert Gordo, and Florent Perronnin. 2012. Iterative quantization: A procrustean approach to learning binary codes for large-scale image retrieval. *IEEE transactions on pattern analysis and machine intelligence* 35, 12 (2012), 2916–2929.

Ian Goodfellow, Jean Pouget-Abadie, Mehdi Mirza, Bing Xu, David Warde-Farley, Sherjil Ozair, Aaron Courville, and Yoshua Bengio. 2014. Generative adversarial nets. In

- NeurIPS*.
- Timofey Grigoryev, Andrey Voynov, and Artem Babenko. 2022. When, Why, and Which Pretrained GANs Are Useful?. In *ICLR*.
- Venkat N Gudivada and Vijay V Raghavan. 1995. Content based image retrieval systems. *Computer* 28, 9 (1995), 18–22.
- David Ha and Jürgen Schmidhuber. 2018. World models. *arXiv preprint arXiv:1803.10122* (2018).
- Ligong Han, Yinxiao Li, Han Zhang, Peyman Milanfar, Dimitris Metaxas, and Feng Yang. 2023. Svdiff: Compact parameter space for diffusion fine-tuning. *arXiv preprint arXiv:2303.11305* (2023).
- Amir Hertz, Ron Mokady, Jay Tenenbaum, Kfir Aberman, Yael Pritch, and Daniel Cohen-Or. 2022. Prompt-to-prompt image editing with cross attention control. *arXiv preprint arXiv:2208.01626* (2022).
- Aaron Hertzmann. 2020. Computers do not make art, people do. *Commun. ACM* 63, 5 (2020), 45–48.
- Martin Heusel, Hubert Ramsauer, Thomas Unterthiner, Bernhard Nessler, and Sepp Hochreiter. 2017. GANs trained by a two time-scale update rule converge to a local Nash equilibrium. In *NeurIPS*.
- Geoffrey E Hinton. 2002. Training products of experts by minimizing contrastive divergence. *Neural computation* 14, 8 (2002), 1771–1800.
- Jonathan Ho, Ajay Jain, and Pieter Abbeel. 2020. Denoising Diffusion Probabilistic Models. In *NeurIPS*.
- Edward J Hu, Yelong Shen, Phillip Wallis, Zeyuan Allen-Zhu, Yuanzhi Li, Shean Wang, Lu Wang, and Weizhu Chen. 2021. Lora: Low-rank adaptation of large language models. *arXiv preprint arXiv:2106.09685* (2021).
- Weiming Hu, Nianhua Xie, Li Li, Xianglin Zeng, and Stephen Maybank. 2011. A survey on visual content-based video indexing and retrieval. *IEEE Transactions on Systems, Man, and Cybernetics, Part C (Applications and Reviews)* 41, 6 (2011), 797–819.
- Xun Huang, Arun Mallya, Ting-Chun Wang, and Ming-Yu Liu. 2022. Multimodal Conditional Image Synthesis with Product-of-Experts GANs. In *ECCV*.
- Wonjong Jang, Gwangjin Ju, Yuchool Jung, Jiaolong Yang, Xin Tong, and Seungyong Lee. 2021. StyleCariGAN: Caricature Generation via StyleGAN Feature Map Modulation. *ACM TOG* (2021).
- Hervé Jégou, Matthijs Douze, Cordelia Schmid, and Patrick Pérez. 2010. Aggregating local descriptors into a compact image representation. In *2010 IEEE computer society conference on computer vision and pattern recognition*. IEEE, 3304–3311.
- Chao Jia, Yinfei Yang, Ye Xia, Yi-Ting Chen, Zarana Parekh, Hieu Pham, Quoc Le, Yun-Hsuan Sung, Zhen Li, and Tom Duerig. 2021. Scaling up visual and vision-language representation learning with noisy text supervision. In *ICML*.
- Andrei Karpathy, Armand Joulin, and Li F Fei-Fei. 2014. Deep fragment embeddings for bidirectional image sentence mapping. In *NeurIPS*.
- Tero Karras, Timo Aila, Samuli Laine, and Jaakko Lehtinen. 2018. Progressive growing of gans for improved quality, stability, and variation. In *ICLR*.
- Tero Karras, Miika Aittala, Janne Hellsten, Samuli Laine, Jaakko Lehtinen, and Timo Aila. 2020a. Training Generative Adversarial Networks with Limited Data. In *NeurIPS*.
- Tero Karras, Miika Aittala, Samuli Laine, Erik Härkönen, Janne Hellsten, Jaakko Lehtinen, and Timo Aila. 2021. Alias-Free Generative Adversarial Networks. In *NeurIPS*.
- Tero Karras, Samuli Laine, and Timo Aila. 2019. A style-based generator architecture for generative adversarial networks. In *CVPR*.
- Tero Karras, Samuli Laine, Miika Aittala, Janne Hellsten, Jaakko Lehtinen, and Timo Aila. 2020b. Analyzing and improving the image quality of stylegan. In *CVPR*.
- Bahjat Kawar, Shiran Zada, Oran Lang, Omer Tov, Huiwen Chang, Tali Dekel, Inbar Mosseri, and Michal Irani. 2023. Imagic: Text-based real image editing with diffusion models. (2023), 6007–6017.
- Diederik P Kingma and Max Welling. 2014. Auto-encoding variational bayes. In *ICLR*.
- Alex Krizhevsky and Geoffrey E Hinton. 2011. Using very deep autoencoders for content-based image retrieval.. In *ESANN*, Vol. 1. Citeseer, 2.
- Nupur Kumari, Bingliang Zhang, Richard Zhang, Eli Shechtman, and Jun-Yan Zhu. 2023. Multi-concept customization of text-to-image diffusion. (2023), 1931–1941.
- Nupur Kumari, Richard Zhang, Eli Shechtman, and Jun-Yan Zhu. 2022. Ensembling Off-the-shelf Models for GAN Training. In *CVPR*.
- Kathleen M Lewis, Srivatsan Varadharajan, and Ira Kemelmacher-Shlizerman. 2021. TryOnGAN: Body-Aware Try-On via Layered Interpolation. *ACM TOG* (2021).
- Junnan Li, Dongxu Li, Caiming Xiong, and Steven Hoi. 2022. BLIP: Bootstrapping Language-Image Pre-training for Unified Vision-Language Understanding and Generation. *arXiv:2201.12086* [cs.CV]
- Yijun Li, Richard Zhang, Jingwan Lu, and Eli Shechtman. 2020. Few-shot image generation with elastic weight consolidation. In *NeurIPS*.
- Yen-Liang Lin, Cheng-Yu Huang, Hao-Jeng Wang, and Winston Hsu. 2013. 3D sub-query expansion for improving sketch-based multi-view image retrieval. In *ICCV*.
- Bingchen Liu, Yizhe Zhu, Kunpeng Song, and Ahmed Elgammal. 2021. Towards faster and stabilized gan training for high-fidelity few-shot image synthesis. In *ICLR*.
- Li Liu, Fumin Shen, Yuming Shen, Xianglong Liu, and Ling Shao. 2017. Deep sketch hashing: Fast free-hand sketch-based image retrieval. In *CVPR*.
- Zhuang Liu, Hanzi Mao, Chao-Yuan Wu, Christoph Feichtenhofer, Trevor Darrell, and Saining Xie. 2022. A convnet for the 2020s. In *Proceedings of the IEEE/CVF conference on computer vision and pattern recognition*. 11976–11986.
- David G Lowe. 2004. Distinctive image features from scale-invariant keypoints. *IJCV* 60, 2 (2004), 91–110.
- lucid layers. 2022. Datasets and pretrained Models for StyleGAN3. https://github.com/edstoisca/lucid_stylegan3_datasets_models/.
- Yiyang Ma, Huan Yang, Wenjing Wang, Jianlong Fu, and Jiaying Liu. 2023. Unified multi-modal latent diffusion for joint subject and text conditional image generation. *arXiv preprint arXiv:2303.09319* (2023).
- Christopher Manning, Prabhakar Raghavan, and Hinrich Schütze. 2010. Introduction to information retrieval. *Natural Language Engineering* 16, 1 (2010), 100–103.
- Ben Mildenhall, Pratul P Srinivasan, Matthew Tancik, Jonathan T Barron, Ravi Ramamoorthi, and Ren Ng. 2021. Nerf: Representing scenes as neural radiance fields for view synthesis. *Commun. ACM* 65, 1 (2021), 99–106.
- Sangwoo Mo, Minsu Cho, and Jinwoo Shin. 2020. Freeze the Discriminator: a Simple Baseline for Fine-Tuning GANs. In *CVPR Workshop*.
- Ron Mokady, Michal Yarom, Omer Tov, Oran Lang, Daniel Cohen-Or, Tali Dekel, Michal Irani, and Inbar Mosseri. 2022. Self-Distilled StyleGAN: Towards Generation from Internet Photos. In *ACM SIGGRAPH*.
- Yotam Nitzan, Kfir Aberman, Qiurui He, Orly Liba, Michal Yarom, Yossi Gandelsman, Inbar Mosseri, Yael Pritch, and Daniel Cohen-Or. 2022. MyStyle: A Personalized Generative Prior. *arXiv preprint arXiv:2203.17272* (2022).
- Atsuhiko Noguchi and Tatsuya Harada. 2019. Image generation from small datasets via batch statistics adaptation. In *ICCV*.
- Utkarsh Ojha, Yijun Li, Cynthia Lu, Alexei A. Efros, Yong Jae Lee, Eli Shechtman, and Richard Zhang. 2021. Few-shot Image Generation via Cross-domain Correspondence. In *CVPR*.
- Aude Oliva and Antonio Torralba. 2001. Modeling the shape of the scene: A holistic representation of the spatial envelope. *IJCV* 42, 3 (2001), 145–175.
- Aaron van den Oord, Nal Kalchbrenner, Oriol Vinyals, Lasse Espeholt, Alex Graves, and Koray Kavukcuoglu. 2016. Conditional Image Generation with PixelCNN Decoders. In *NeurIPS*.
- Aaron van den Oord, Yazhe Li, and Oriol Vinyals. 2018. Representation learning with contrastive predictive coding. *arXiv preprint arXiv:1807.03748* (2018).
- Gaurav Parmar, Richard Zhang, and Jun-Yan Zhu. 2022. On Buggy Resizing Libraries and Surprising Subtleties in FID Calculation. In *CVPR*.
- Or Patashnik, Zongze Wu, Eli Shechtman, Daniel Cohen-Or, and Dani Lischinski. 2021. Styleclip: Text-driven manipulation of stylegan imagery. In *ICCV*. 2085–2094.
- Justin Pinkney. 2020. Awesome Pretrained StyleGAN. <https://www.justinpinkney.com/pretrained-stylegan/>.
- Ben Poole, Ajay Jain, Jonathan T Barron, and Ben Mildenhall. 2022. Dreamfusion: Text-to-3d using 2d diffusion. *arXiv preprint arXiv:2209.14988* (2022).
- Filip Radenovic, Giorgos Tolias, and Ondrej Chum. 2018. Deep shape matching. In *ECCV*.
- Alec Radford, Jong Wook Kim, Chris Hallacy, Aditya Ramesh, Gabriel Goh, Sandhini Agarwal, Girish Sastry, Amanda Askell, Pamela Mishkin, Jack Clark, Gretchen Krueger, and Ilya Sutskever. 2021. Learning transferable visual models from natural language supervision. In *ICML*.
- Aditya Ramesh, Prafulla Dhariwal, Alex Nichol, Casey Chu, and Mark Chen. 2022. Hierarchical text-conditional image generation with clip latents. *arXiv preprint arXiv:2204.06125* (2022).
- Ali Razavi, Aaron van den Oord, and Oriol Vinyals. 2019. Generating diverse high-fidelity images with vq-vae-2. In *NeurIPS*.
- Leo Sampaio Ferraz Ribeiro, Tu Bui, John Collomosse, and Moacir Ponti. 2020. Sketch-former: Transformer-based representation for sketched structure. In *CVPR*.
- Robin Rombach, Andreas Blattmann, Dominik Lorenz, Patrick Esser, and Björn Ommer. 2022. High-Resolution Image Synthesis with Latent Diffusion Models. In *CVPR*.
- Natanuel Ruiz, Yuanzhen Li, Varun Jampani, Yael Pritch, Michael Rubinstein, and Kfir Aberman. 2022. DreamBooth: Fine Tuning Text-to-image Diffusion Models for Subject-Driven Generation. In *arXiv preprint arXiv:2208.12242*.
- Chitwan Saharia, William Chan, Saurabh Saxena, Lala Li, Jay Whang, Emily L Denton, Kamyar Ghasemipour, Raphael Gontijo Lopes, Burcu Karagol Ayan, Tim Salimans, et al. 2022. Photorealistic text-to-image diffusion models with deep language understanding. *Advances in Neural Information Processing Systems* 35 (2022), 36479–36494.
- Patsorn Sangkloy, Nathan Burnell, Cusuh Ham, and James Hays. 2016. The sketchy database: learning to retrieve badly drawn bunnies. *ACM TOG* 35, 4 (2016), 1–12.
- Axel Sauer, Kashyap Chitta, Jens Müller, and Andreas Geiger. 2021. Projected GANs Converge Faster. In *NeurIPS*.
- Axel Sauer, Katja Schwarz, and Andreas Geiger. 2022. Stylegan-xl: Scaling stylegan to large diverse datasets. In *ACM SIGGRAPH*.
- Derrick Schultz. 2020. FreaGAN, undertrained GAN trained on Frea Buckler’s artwork. <https://twitter.com/dvsch/status/1255885874560225284>.
- Yongliang Shen, Kaitao Song, Xu Tan, Dongsheng Li, Weiming Lu, and Yueting Zhuang. 2023. Hugginggpt: Solving ai tasks with chatgpt and its friends in huggingface. *arXiv preprint arXiv:2303.17580* (2023).
- Josef Sivic and Andrew Zisserman. 2003. Video Google: A text retrieval approach to object matching in videos. In *ICCV*.

- Arnold WM Smeulders, Marcel Worring, Simone Santini, Amarnath Gupta, and Ramesh Jain. 2000. Content-based image retrieval at the end of the early years. *IEEE TPAMI* (2000).
- Richard Socher, Andrej Karpathy, Quoc V Le, Christopher D Manning, and Andrew Y Ng. 2014. Grounded compositional semantics for finding and describing images with sentences. *Transactions of the Association for Computational Linguistics* 2 (2014), 207–218.
- Jiaming Song, Chenlin Meng, and Stefano Ermon. 2021a. Denoising diffusion implicit models. In *ICLR*.
- Yang Song, Jascha Sohl-Dickstein, Diederik P Kingma, Abhishek Kumar, Stefano Ermon, and Ben Poole. 2021b. Score-based generative modeling through stochastic differential equations. In *ICLR*.
- A. Tewari, O. Fried, J. Thies, V. Sitzmann, S. Lombardi, K. Sunkavalli, R. Martin-Brualla, T. Simon, J. Saragih, M. Nießner, R. Pandey, S. Fanello, G. Wetzstein, J.-Y. Zhu, C. Theobalt, M. Agrawala, E. Shechtman, D. B Goldman, and M. Zollhöfer. 2020. State of the Art on Neural Rendering. *Computer Graphics Forum (EG STAR 2020)* (2020).
- Antonio Torralba, Rob Fergus, and Yair Weiss. 2008. Small codes and large image databases for recognition. In *CVPR*.
- Narek Tumanyan, Michal Geyer, Shai Bagon, and Tali Dekel. 2023. Plug-and-play diffusion features for text-driven image-to-image translation. In *Proceedings of the IEEE/CVF Conference on Computer Vision and Pattern Recognition. 1921–1930*.
- Unsplash. 2022. Unsplash. <https://unsplash.com>.
- Sheng-Yu Wang, David Bau, and Jun-Yan Zhu. 2021. Sketch Your Own GAN. In *ICCV*.
- Sheng-Yu Wang, David Bau, and Jun-Yan Zhu. 2022. Rewriting Geometric Rules of a GAN. *ACM TOG* (2022).
- Yaxing Wang, Abel Gonzalez-Garcia, David Berga, Luis Herranz, Fahad Shahbaz Khan, and Joost van de Weijer. 2020. Minegan: effective knowledge transfer from gans to target domains with few images. In *CVPR*.
- Yaxing Wang, Chenshen Wu, Luis Herranz, Joost van de Weijer, Abel Gonzalez-Garcia, and Bogdan Raducanu. 2018. Transferring gans: generating images from limited data. In *ECCV*.
- Yair Weiss, Antonio Torralba, and Rob Fergus. 2008. Spectral hashing. In *NeurIPS*.
- Fisher Yu, Ari Seff, Yinda Zhang, Shuran Song, Thomas Funkhouser, and Jianxiong Xiao. 2015. Lsun: Construction of a large-scale image dataset using deep learning with humans in the loop. *arXiv preprint arXiv:1506.03365* (2015).
- Qian Yu, Feng Liu, Yi-Zhe Song, Tao Xiang, Timothy M Hospedales, and Chen-Change Loy. 2016. Sketch me that shoe. In *CVPR*.
- Lvmin Zhang, Anyi Rao, and Maneesh Agrawala. 2023. Adding conditional control to text-to-image diffusion models. In *Proceedings of the IEEE/CVF International Conference on Computer Vision. 3836–3847*.
- Yuxuan Zhang, Huan Ling, Jun Gao, Kangxue Yin, Jean-Francois Lafleche, Adela Barriuso, Antonio Torralba, and Sanja Fidler. 2021. Datasetgan: Efficient labeled data factory with minimal human effort. In *CVPR*.
- Miaoyun Zhao, Yulai Cong, and Lawrence Carin. 2020a. On leveraging pretrained GANs for generation with limited data. In *ICML*.
- Shengyu Zhao, Zhijian Liu, Ji Lin, Jun-Yan Zhu, and Song Han. 2020b. Differentiable Augmentation for Data-Efficient GAN Training. In *NeurIPS*.
- Liang Zheng, Yi Yang, and Qi Tian. 2017. SIFT meets CNN: A decade survey of instance retrieval. *IEEE TPAMI* (2017).
- Peihao Zhu, Rameen Abdal, John Femiani, and Peter Wonka. 2021. Barbershop: Gan-based image compositing using segmentation masks. *ACM TOG* (2021).

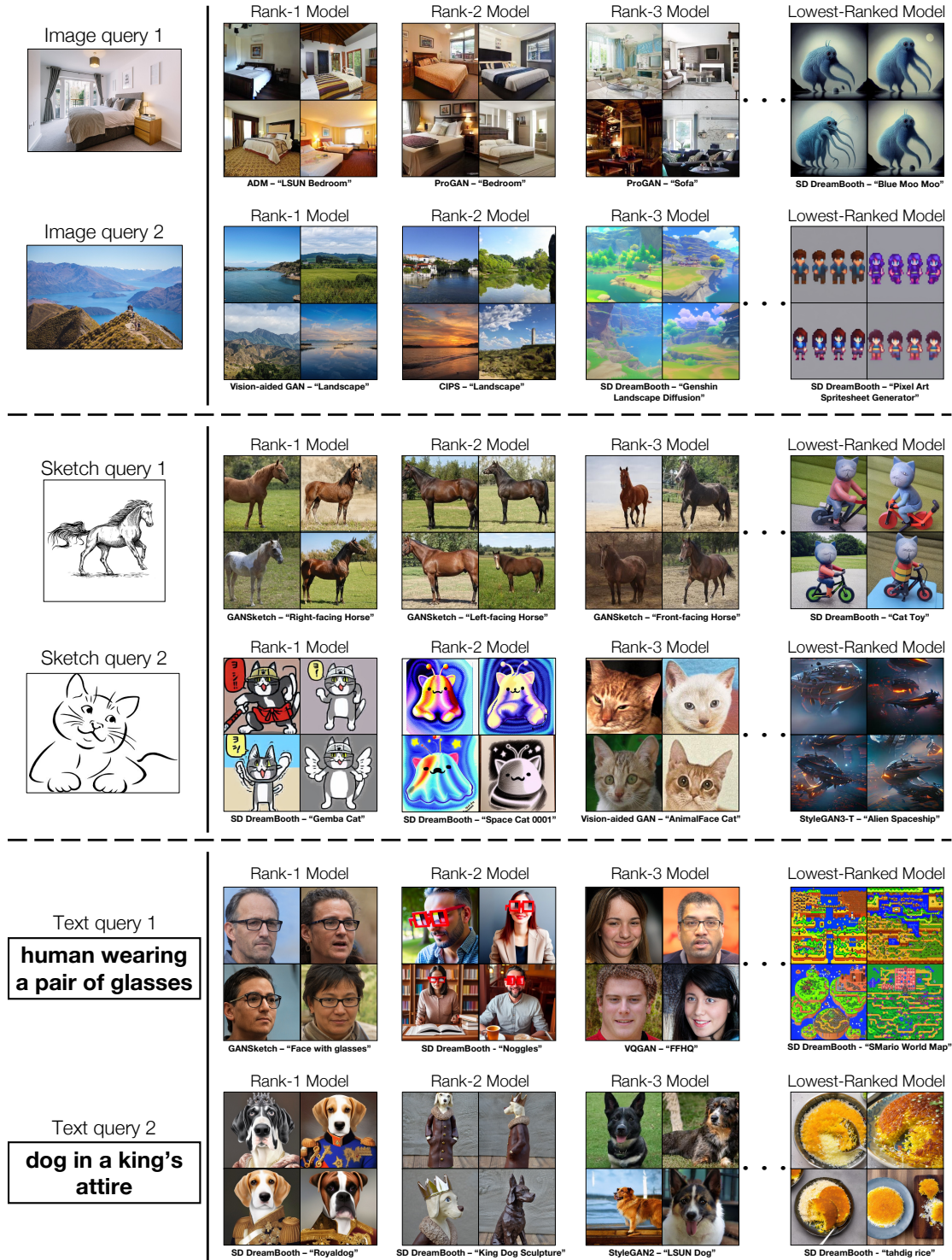


Fig. 7. **Qualitative results of model retrieval.** *Top row (image query):* Our algorithm retrieves matching models of indoor scenes and landscapes. *Middle row (sketch query):* Animal sketches retrieve other animals, and more simplistic sketches (e.g. the cat sketch) tend to retrieve cartoonish models. *Bottom row (text query):* We retrieve relevant models matching the textual description. Photos by Stuart Bailey and @timbri97 on Pixabay. Sketches by Damaris Dharmah and @OpenClipart-Vectors on Pixabay.

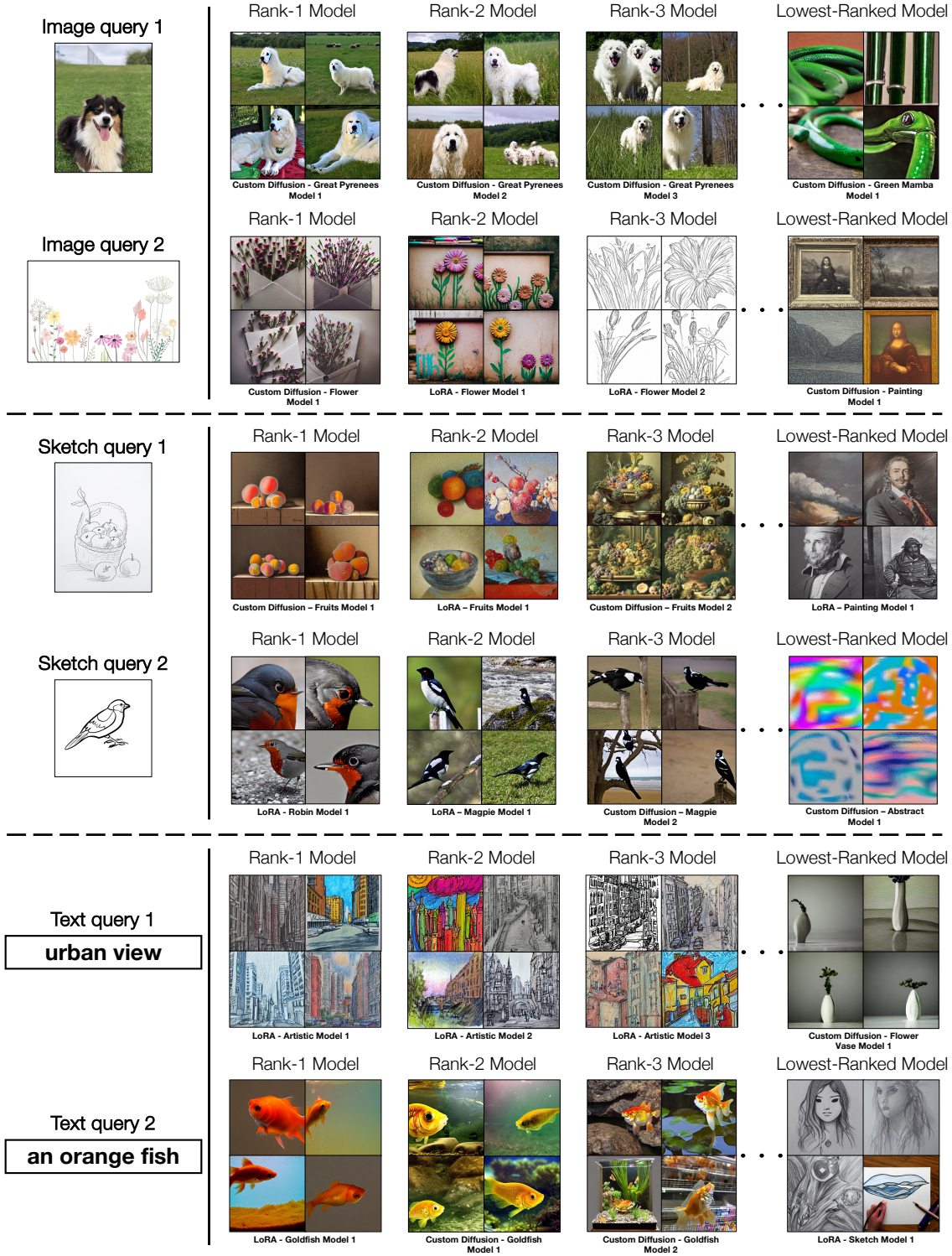


Fig. 8. **Qualitative results of model retrieval on Synthetic Model Zoo.** Top row (image query): Our algorithm retrieves models of the dog breed Great Pyrenees and artistic flowers, given matching image queries. Middle row (sketch query): Given sketches of a fruit basket and a bird, our algorithm retrieves models that generate a collection of fruits, and other birds, respectively. Bottom row (text query): We can also retrieve relevant models with a textual description. Images by @drcaringola and @Owantana on Pixabay. Sketches by @N-region and @Tilixia on Pixabay.

APPENDIX

Overview. In Section A, we run additional tests that reveal our method’s retrieval score distribution, variance, run-time, and memory profile. In Section B, we describe the Generative Model Zoo details. In Section C, we derive our Monte-Carlo and 1st Moment model retrieval baselines from a probabilistic perspective. Section D discusses potential negative social impacts and social benefits associated with the applications of our model retrieval algorithm. Our code, data, and models will be available upon publication.

A ADDITIONAL ANALYSIS

Cross Validation on Internet Model Zoo. We perform 5-fold cross-validation on the Internet Model Zoo and find that fine-tuning improves model retrieval accuracy compared to pre-trained counterparts. We show results in Table 5. The finding is consistent with when we run cross-validation on the Synthetic Model Zoo (Table 1).

Distribution of retrieval scores. We plotted the top-1-to-10 retrieval scores with the 1st Moment method (eq. 12) for a few text queries in Figure 9. For more specific queries like “a bird that talks” (describing the parrot, a type of bird), “edvard munch” (a painter’s name), or “buses”, the 1st Moment similarity scores show a clear drop between relevant and irrelevant models. On the other hand, more general queries like “animals” or “animated faces” can have many relevant models, so the similarity scores appear more uniform. If a query has no good matches, as is the case with “coffee cup”, the similarity scores also appear uniform.

Evaluation with mean average precision. Table 6 reports the performance of baseline and our fine-tuned methods for model retrieval using mean average precision as the evaluation metric.

Run-time and memory analysis. We profile our methods’ running time and memory usage on 259 generative models as well as a much greater number of models in simulation. To simulate models, we sample the 1st Moment model statistics and Monte-Carlo samples from a 512-dimensional normal distribution that correspond to points in the CLIP feature space, and the second moment statistics are generated as a unit covariance matrix with a small, uniform, symmetric noise added. We store the statistics needed for the respective method in the GPU’s VRAM during model retrieval. We run the following tests on a machine equipped with an AMD Threadripper 3960X and NVIDIA RTX A5000 running Pytorch 1.11.0, and report the runtimes in Table 7.

During model retrieval, extracting query features takes constant time regardless of the number of models to retrieve. In the case of text, extracting CLIP features takes 5.02 ms and 0.36 GB of VRAM. Even for one million models, the 1st Moment based scoring method only takes 0.19 ms and 1.93 GB of VRAM. When handling image-to-model or sketch-to-model retrieval, extracting query features with CLIP takes 6.75 ms and 0.36 GB of VRAM. Compared to 1st Moment, the Gaussian Density method requires extra memory to store the models’ covariance matrices. With 10,000 models, Gaussian Density takes 0.49ms and 9.85 GB of VRAM. Switching to the 1st Moment method offers a $3.06 \times$ speed up and a $458 \times$ reduction in memory consumption while achieving a similar accuracy (see Table 1). Using the fine-tuned 1st Moment improves accuracy, but roughly doubles the running time due to the matrix multiplication

Table 5. **Cross validation on Internet Model Zoo.** We fine-tune different combinations of scoring function and transformation matrix parameterization with 5-fold cross-validation on the Internet Model Zoo. The best-performing parameterization of A_ψ for each scoring method by modality is marked with a “★”.

	Modality	A_ψ	Mean Testing Accuracy		
			Top-1 (FT)	Top-1 (Pre-trained)	
Internet Zoo	CLIP+1 st Moment	Image	Diagonal	0.92	0.91
	CLIP+1 st Moment	Image	★Triangular	0.94	0.91
	CLIP+1 st Moment	Image	Full	0.92	0.91
	CLIP+Gaussian Density	Image	★Diagonal	0.95	0.94
	CLIP+Gaussian Density	Image	Triangular	0.93	0.94
	CLIP+Gaussian Density	Image	Full	0.92	0.94
	CLIP+1 st Moment	Sketch	Diagonal	0.60	0.55
	CLIP+1 st Moment	Sketch	★Triangular	0.75	0.55
	CLIP+1 st Moment	Sketch	Full	0.72	0.55
	CLIP+Gaussian Density	Sketch	★Diagonal	0.57	0.35
	CLIP+Gaussian Density	Sketch	Triangular	0.46	0.35
	CLIP+Gaussian Density	Sketch	Full	0.40	0.35

Table 6. **mAP numbers.** We report the performance of baseline and our fine-tuned methods for model retrieval using mean average precision as the evaluation metric. For top-K accuracy numbers, see main text Table 1.

	Image (Gen.)	Sketch
CLIP+Monte-Carlo (2.4K)	0.88	0.45
CLIP+best-k (2.4K, k=1)	0.87	0.41
CLIP+best-k (2.4K, k=10)	0.88	0.45
CLIP+1 st Moment	0.85	0.45
CLIP+1 st Moment (FT)	0.87	0.61
CLIP+Gaussian Density	0.89	0.29
CLIP+Gaussian Density (FT)	0.90	0.42

Table 7. **Model retrieval running time.** The table shows the running time of different retrieval methods. OOM stands for “out of memory” on a 24GB-VRAM GPU and that the retrieval cannot be done in a single pass. After we get the score for each model, we additionally run `torch.argsort` to get the best matches, which takes 0.03, 0.15, and 0.12 ms for 259, 10K, and one million models, respectively (not shown in the table).

	Feature Extraction	Model Scoring		
		259	10K	1M
Text	Monte-Carlo (2.4K)	0.19ms	OOM	OOM
	1 st Moment	0.09ms	0.16ms	0.21ms
	1 st Moment(FT)	0.17ms	0.30ms	0.33ms
Image	Monte-Carlo (2.4K)	0.19ms	OOM	OOM
	Gaussian Density	0.45ms	0.49ms	OOM
	Gaussian Density(FT)	6.75ms	0.45ms	0.49ms
	1 st Moment	0.06ms	0.15ms	0.19ms
	1 st Moment(FT)	0.15ms	0.28ms	0.32ms

involved. Using the fine-tuned Gaussian Density method also improves accuracy, but comes at no additional computational costs since the covariance matrices can be multiplied with the transformation and cached into memory. The transformation A_ψ is a 512×512 matrix and takes negligible memory to store.

After getting the retrieval scores, the time required for sorting and selecting the most relevant models is comparatively short on

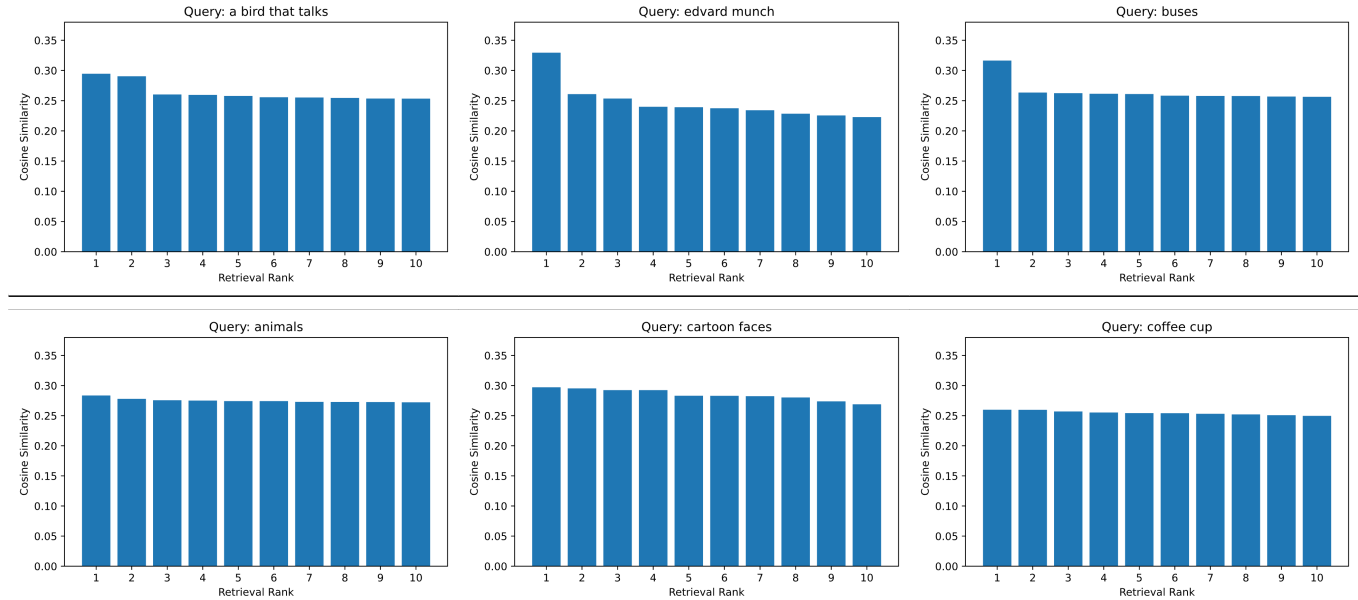


Fig. 9. **Similarity score drop-off.** *Top:* 1st Moment similarity scores of more specific queries like “a bird that talks”, “edvard munch”, or “buses” show a clear drop between relevant and irrelevant models. In the first case, the parrot model was ranked top, closely followed by the bird model. In “edvard munch”, the StyleGAN-NADA Edvard Munch-style face model was ranked top. Subsequent ranks consist of other photorealistic and artistic face models. In “buses”, the ProGAN bus model was ranked top. Subsequent ranks consisted of models that generate trains, faces, and bridges. *Bottom:* for more general queries like “animals” or “animated faces”, or a query like “coffee cup” that does not have any good matches, the similarity scores appear more uniform. In “animals”, the 10 retrieved models generate animals, including sheep, dogs, cows, horses, cats, and giraffes. In “cartoon faces”, we find 8 painting/sketch/cartoon-style face models and 2 photorealistic face models. In “coffee cup”, since our collection does not include any highly relevant models, we find a broad variety of models. The retrieved models consist of a “bottle” model, a modern art painting model, a cat model, a “tryphobia” model, two modern art painting models, two anime/cartoon character models, and two face models.

Table 8. **Model search with fewer-sample statistics.** We run model search while using fewer samples to compute the feature-space image statistics for each model at test-time. “ALL” refers to using all 50K or 2,400 available samples depending on the model, which is the default (see Section B). In other tests we randomly sample a subset of given size.

	Modality	Stats Sample Size	Mean Testing Accuracy		
			Top-1 (FT)	Top-1 (Pre-trained)	
Internet Zoo	CLIP+Gaussian Density	Image	ALL	0.85	0.84
	CLIP+Gaussian Density	Image	2,400	0.85	0.84
	CLIP+Gaussian Density	Image	100	0.79	0.78
	CLIP+Gaussian Density	Image	10	0.68	0.66
	CLIP+1 st Moment	Sketch	ALL	0.49	0.32
	CLIP+1 st Moment	Sketch	2,400	0.49	0.32
	CLIP+1 st Moment	Sketch	100	0.46	0.30
	CLIP+1 st Moment	Sketch	10	0.40	0.27

a GPU. For one million models, sorting takes 0.12ms and 0.062 GB of VRAM. When we use the 1st Moment method, we enable a user to retrieve models from a 1-million-model collection with a text, sketch, or image query in under 10 ms.

Model Search with Fewer-sample Model Statistics. To study how well model search works if model statistics were gathered from fewer generated images, at test-time, we use only a portion of the generated images to compute the feature-space mean and covariance statistics, while keeping all else the same. We show the results in

Table 8. Overall, while a greater sample size helps, we get adequate performance with as few as 100 samples.

Evaluation over multi-modal queries. To test retrieval with multi-modal (image + text) queries, we select a subset of 36 models from the Internet Model Zoo whose description can be split into some text and a generic image (e.g., “purple fur” + image of a regular horse, for a purple horse model). Our CLIP+1st Moment method results in 0.47 and 0.86 for top-1 and top-5 accuracies. The qualitative results are presented in Figure 10.

Refined search using spatial features. As shown in Figure 6 in the main paper, our method sometimes fails when there is a directional dependency, e.g., left-facing vs. right-facing horse models. To this end, we experiment with spatial features. Given 50 image queries of left- and right-facing horses (identical images, flipped), we take 7x7 spatial features from the last layer of ConvNext [Liu et al. 2022] pre-trained on ImageNet-22k and see if each query retrieves the left- or the right-facing-horse model. The horse model facing the same direction as the query is favored 100% of the time using spatial features and the 1st Moment method. In contrast, 1st Moment (pre-trained), 1st Moment (fine-tuned), Gaussian Density (pre-trained), and Gaussian Density (fine-tuned) methods favor the correct model 52%, 52%, 49% and 54% of the time, respectively.

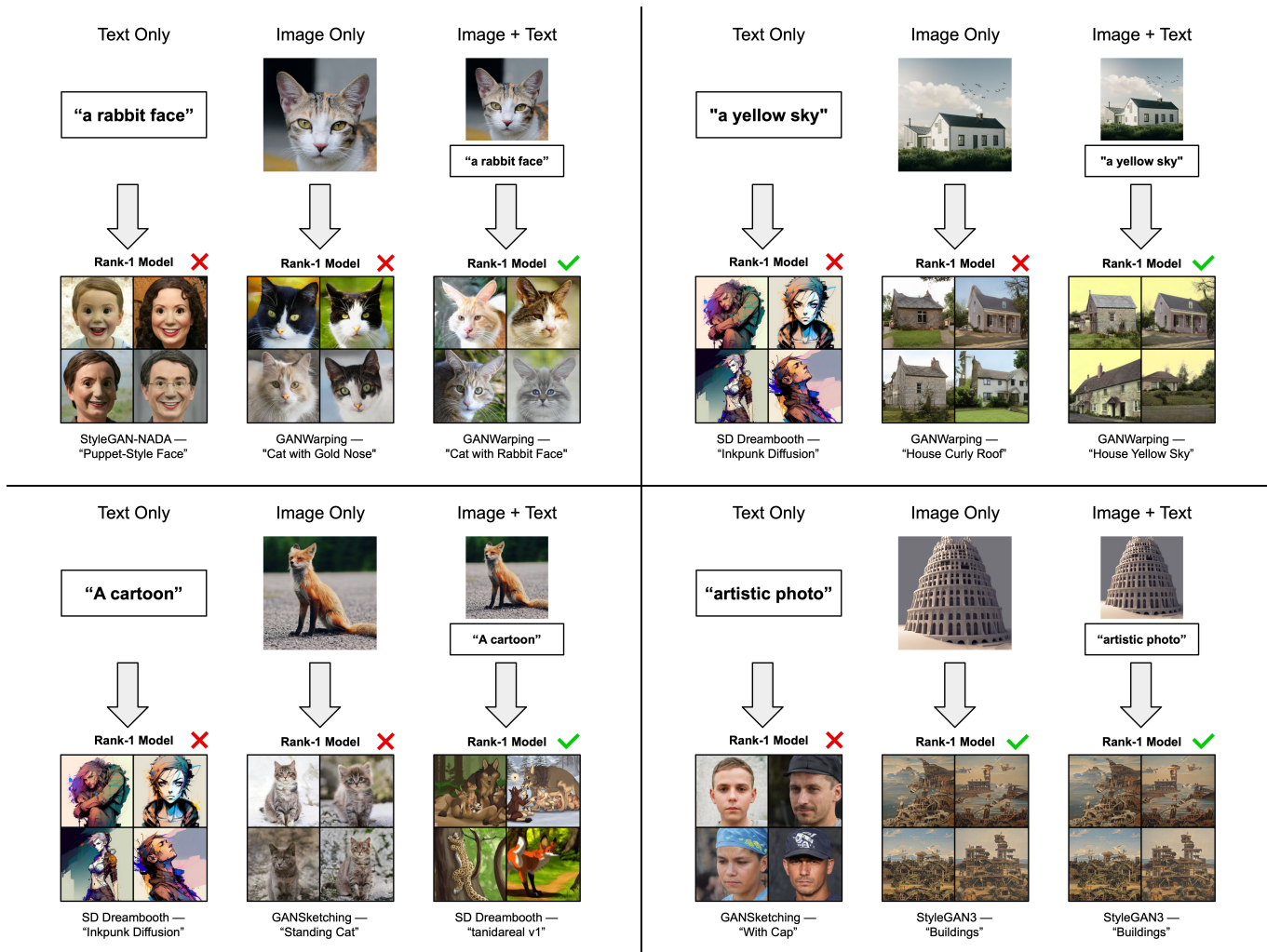


Fig. 10. **Evaluation over multi-modal queries.** We show the qualitative results of retrieval using text only, image only, and image + text as the query. We search over a subset of the Internet Model Zoo, specifically, we selected 36 models whose descriptions can be split into text and image. We can utilize direction from both text and image to retrieve models more consistently. Photos by Himanshu Choudhary, Alexander Andrews, and Qijin Xu on Unsplash. Rendering by @ForgottenWorld on Blender Artists (bottom right).

Figure 11 shows a qualitative comparison between using spatial features vs. global CLIP features when retrieving left and right-facing horse models with our Gaussian Density (fine-tuned) method. Model search with global CLIP features retrieves the right-facing horse model even though the query depicted a left-facing horse (Figure 11, last column), where we retrieve the correct model with spatial features.

B DATASET DETAILS

Distribution of Models within Generative Model Zoo. The 259 models in Internet Model Zoo consist of 1 ADM model [Dhariwal and Nichol 2021], 3 CIPS [Anokhin et al. 2021], 2 DDIM [Song et al. 2021a], 2 DDPM [Ho et al. 2020], 1 FastGAN [Liu et al. 2021], 18 GANWarping [Wang et al. 2022], 14 GANSketching [Wang et al. 2021], 31 ProGAN [Karras et al. 2018], 7 Self-Distilled GAN [Mokady

et al. 2022], 2 StyleGAN-XL [Sauer et al. 2022], 2 VQGAN [Esser et al. 2021], 10 Vision-Aided GAN [Kumari et al. 2022], 21 StyleGAN-2 [Karras et al. 2020b], 17 StyleGAN-3 [Karras et al. 2021], 20 StyleGAN-NADA [Gal et al. 2022b] models, and 108 DreamBooth [Ruiz et al. 2022] fine-tuned Stable-Diffusion models.

Model statistics calculation. For the Internet Model Zoo, we use 50K generated images to pre-calculate the sample mean and covariance, except for the 108 DreamBooth fine-tuned Stable-Diffusion models where we use 2,400 generated images. In the case of Synthetic Model Zoo, we sample 2400 images to calculate the model statistics, as it consists of 1000 customized diffusion models sampling from which is computationally inefficient. We always add a small factor ($1e^{-4}$) of the identity matrix to the covariance estimate to improve numerical stability. For ImageNet fine-tuned models,

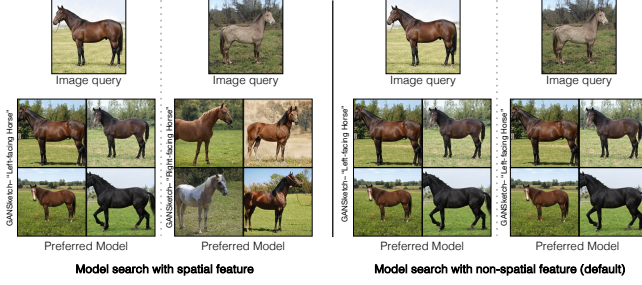


Fig. 11. **Refined model retrieval with respect to the spatial layout of the query.** We compare image-based model retrieval using the last layer 7x7 spatial features from ConvNext [Liu et al. 2022] pretrained on ImageNet-22k (1st Moment method) vs. using global CLIP features (Gaussian Density(FT) method). In the last column, the search with global features fails to retrieve the model facing the same direction as the query, whereas the search with spatial features retrieves the correct model in both cases shown.

we generate class-specific prompts used to sample images using ChatGPT with the instruction: “Generate 32 captions for images containing a <class-name>. The caption should also contain the word <class-name>”. For artistic fine-tuned models, we use the following two prompts: “a painting in the style of <specific art style>” and “a drawing in the style of <specific art style>”.

Generating Image and Sketch Queries. For every model, we generate 50 more images with the same hyperparameters as used to generate images that are used to compute its distribution statistics. We then create sketches queries by synthesizing sketches from the image queries using the method of Chan *et al.* [2022].

C DERIVATION FOR TEXT-BASED MODEL RETRIEVAL

Monte Carlo Estimation. Given a text query q and a generative model $p(x|\theta)$ capturing a distribution of images x , we want to estimate the conditional probability $p(q|\theta)$.

$$\begin{aligned} p(q|\theta) &= \int p(q, x|\theta) dx = \int p(q|x)p(x|\theta) dx \\ &= \int \frac{p(x|q)p(q)}{p(x)} p(x|\theta) dx \propto \int \frac{p(x|q)}{p(x)} p(x|\theta) dx \end{aligned} \quad (7)$$

Here we assume conditional independence between query q and model θ given image x (i.e., $p(q|x, \theta) = p(q|x)$), since the same image x should match the same set of queries regardless of the model choice. We apply Bayes’ rule in the second line of Equation 7 to get the final expression. In Equation 7, a text query q may correspond to multiple possible image matches $p(x|q)$, and we estimate the term $\frac{p(x|q)}{p(x)}$ using cross-modal similarities. In fact, this expression is proportional to the score function f in contrastive learning (e.g., InfoNCE [Oord et al. 2018]), where $f(x, q) \propto \frac{p(x|q)}{p(x)}$. Since CLIP [Radford et al. 2021] is trained on a text-image retrieval task with the InfoNCE loss, we can directly apply the pre-trained CLIP model to simplify Equation 7.

$$\max_{\theta \in \{\theta_1, \dots, \theta_N\}} \int p(x|\theta) f(x, q) dx = \mathbb{E}_{x \sim p(x|\theta)} [f(x, q)]. \quad (8)$$

We recall that CLIP consists of an image encoder ϕ_{im} and a text encoder ϕ_{txt} , and it is trained with a score function based on cosine similarity:

$$f(x, q) = \exp\left(\frac{h_x^T h_q}{\tau(\|h_x\| \cdot \|h_q\|)}\right) = \exp\left(\frac{\tilde{h}_x^T \tilde{h}_q}{\tau}\right), \quad (9)$$

where $h_x := \phi_{\text{im}}(x)$ and $h_q := \phi_{\text{txt}}(q)$ are the image and text feature from CLIP, respectively. $\tilde{h}_x = \frac{h_x}{\|h_x\|}$ and $\tilde{h}_q = \frac{h_q}{\|h_q\|}$ are the normalized features. Hence, Equation 9 can be written precisely as:

$$\max_{\theta \in \{\theta_1, \dots, \theta_N\}} \mathbb{E}_{h_x \sim p(h_x|\theta)} \left[\exp\left(\frac{\tilde{h}_x^T \tilde{h}_q}{\tau}\right) \right] \quad (10)$$

Even though we cannot compute the expectation inside Equation 10 in closed form, we can estimate this quantity by sampling from $p(h_x|\theta)$ and computing an empirical average. We call this method Monte-Carlo. To further speed up model retrieval, we provide an approximation for Equation 10 – the 1st Moment method.

1st Moment Method. We derive a point estimation at the first moment of the model distribution. Specifically, we estimate the mean of the normalized CLIP image features. (Since CLIP features are learned to be magnitude-invariant, we normalize CLIP features in all of our methods.) Here, we can approximate the feature distribution using a Dirac delta function, where $p(h_x|\theta) \sim \delta(h_x - \mu_n)$. μ_n is the first moment of the distribution, where $\mu_n = \mathbb{E}_{h_x \sim p(h_x|\theta)} [h]$. With this approximation, we can rewrite Equation 10 as:

$$\max_{\theta \in \{\theta_1, \dots, \theta_N\}} \exp\left(\frac{\tilde{\mu}_n^T \tilde{h}_q}{\tau}\right) \quad (11)$$

$$\text{where } \mu_n = \left(\mathbb{E}_{h_x \sim p(h_x|\theta)} [h_x]\right); \tilde{\mu}_n = \frac{\mu_n}{\|\mu_n\|}$$

Since the exponential mapping and temperature mapping are monotonically increasing functions, we can further simplify the expression to be our 1st Moment method:

$$\max_{\theta \in \{\theta_1, \dots, \theta_N\}} \tilde{\mu}_n^T \tilde{h}_q \quad (12)$$

$$\text{where } \mu_n = \left(\mathbb{E}_{h_x \sim p(h_x|\theta)} [h_x]\right); \tilde{\mu}_n = \frac{\mu_n}{\|\mu_n\|}$$

D SOCIETAL IMPACT

Our method is a step towards making the plethora of generative models cropping up nowadays available to users with ease. However, model search could be used in negative ways: simplifying access to many models may make it easier for malicious actors to create fake content that is difficult to distinguish from real photos. The efficient search may also make it easier to distribute or locate private, offensive, or other damaging information from within a large set of pre-trained models. For that reason, we believe it is important for a model search index to maintain a code of conduct for users and contributors. On the other hand, developing effective model search methods has potential benefits: it may help reduce errors that result from using the wrong model for a problem; it may be a resource for identifying sources of fakes; and it potentially reduces the resources

consumed by training redundant models when a good model for a problem already exists.